0026-895X/96/051118-09$3.00/0

MOLECULAR PHARMACOLOGY, 50:1118–1126 (1996).

Identification of Critical Extracellular Loop Residues Involved in α_1-Adrenergic Receptor Subtype-Selective Antagonist Binding

MING-MING ZHAO, JOHN HWA,[1] and DIANNE M. PEREZ

Department of Molecular Cardiology, Cleveland Clinic Research Institute, Cleveland, Ohio 44195

Received May 28, 1996; Accepted July 17, 1996

SUMMARY

α_1-Adrenergic receptor (AR) subtypes mediate many effects of the sympathetic nervous system. Although structurally similar, the three cloned subtypes (α_{1a}-AR, α_{1b}-AR, and α_{1d}-AR) bind a series of ligands with different relative potencies. This is particularly true for the α_{1a}-AR, which recognizes a number of ligands with 10–100-fold higher affinity than the α_{1b} or α_{1d} subtypes. Because ligands are hypothesized to bind to receptor residues that are located in the transmembrane (TM) spanning domains, subtype differences in ligand recognition are likely the result of differences in the binding properties of nonconserved TM residues. We previously reported on the identification of two TM residues in the α_{1b}-AR that converted the agonist binding profile entirely to that of the α_{1a}-AR when mutated to corresponding α_{1a}-AR residues. We now report on the determinants of antagonist selectivity between these two α_1-AR subtypes. Construction of a chimera in which the entire fifth TM and a portion of the putative second extracellular loop of the hamster α_{1b}-AR was replaced with the corresponding region of the rat α_{1a}-AR revealed that the chimera accounted for all of the higher binding affinity (8–29-fold) seen in the α_{1a}-AR for two antagonists, phentolamine and WB4101. Using site-directed mutagenesis, we further analyzed individual point mutations making up this chimera. We found that three adjacent residues, which were located on the extracellular loop of the fifth TM, are fully responsible for this higher antagonist binding affinity in the α_{1a}-AR. These three point mutations (G196Q, V197I, T198N) in the α_{1b}-AR were additive and sufficient in their effects on changing antagonist-binding profiles to that of the α_{1a}-AR. Reversal of these three residues in the α_{1a}-AR to their corresponding residues in the α_{1b}-AR completely reversed the antagonist affinity to wild-type α_{1b}-AR values. To aid in molecular modeling, the use of organic chemicals that mimic key structures of the antagonists were used in competitive ligand-binding studies with the mutated receptors. These results indicated the orientation of both phentolamine and WB4101 in the α_1-AR binding pocket. Together, the data indicate that α_1-antagonists may bind near the surface of the receptor, much like the peptide hormone receptors, and not deep within the TM regions, where the ligand-binding pocket was first proposed and identified for α_1 agonists.

α_1-ARs are members of the G protein-coupled receptor superfamily that is activated by the neurotransmitter norepinephrine, which is released from sympathetic nerve endings, and by the neurohormone epinephrine, which is released from the adrenal medulla (1).[2] They are related to a larger subset of catecholamine-binding receptors that includes the β-ARs (e.g., β_1, β_2, β_3) and α_2-ARs (e.g., α_{2a}, α_{2b}, α_{2c}). Three α_1-AR subtypes have been cloned and pharmacologically characterized: α_{1a} (2, 3), α_{1b} (4), and α_{1d}-AR (5, 6). Each α_1-AR subtype has a distinct pharmacology that is recognized through the use of selective ligands. The α_{1a} subtype has 10–100-fold higher affinity for a number of agonists, such as methoxamine, oxymetazoline, and cirazoline, and for a number of antagonists, such as WB4101, phentolamine, 5-methylurapidil, and (+)-niguldipine, compared with the α_{1b} subtype (2). Selective ligands for the α_{1d} subtype include the antagonist BMY 7378 (7) and for the α_{1b} subtype include the selective agonist AH 11110A (8) or cyclazosin (9). However, based on 1000-fold differences in affinity, there are no useful subtype-selective drugs readily available that can fully discriminate among the subtypes.

Recent studies have indicated that α_1 subtypes can mediate important pathways in the development of pathology. In particular, α_{1a}-AR overstimulation in isolated cardiac myocytes seems to promote cardiac hypertrophy and can be reversed through the administration of nonselective α_1 antag-

This work was supported in part by National Institutes of Health Grant RO1-HL52544 (D.M.P.) and an unrestricted research grant from Glaxo Wellcome (D.M.P.).

[1] Current affiliation: Department of Biology and Chemistry, Massachusetts Institute of Technology, Cambridge, MA 02139.

[2] We used the standardized nomenclature system for α_1-AR subtypes as recommended by the International Union of Pharmacology Committee on the Classification of Adrenergic Receptors. The cloned subtypes are designated lowercase letters as α_{1a}, α_{1b}, and α_{1d}. The pharmacologically described tissue subtypes are defined as α_{1A}, α_{1B}, and α_{1D}, respectively (1).

ABBREVIATIONS: AR, adrenergic receptor; [^{125}I]HEAT, 2-[β-(4-hydroxyl-3-[^{125}I]iodophenyl)ethylamineomethyl]tetralone; TM, transmembrane; EGTA, ethylene glycol bis(β-aminoethyl ether)-*N*,*N*,*N*′,*N*′-tetraacetic acid; HEPES, 4-(2-hydroxyethyl)-1-piperazineethanesulfonic acid; PCR, polymerase chain reaction.

onists (10). In addition, the use of nonselective α_1 antagonists for benign prostatic hypertrophy is a current therapy (11) even though it seems that the α_{1a} subtype controls the predominant dynamic component in symptomatic benign prostatic hypertrophy (12). Because of α_1-AR distribution in the vasculature, the use of nonselective drugs increases the propensity for side effects, such as hypotension, which is a common effect of the nonselective α_1-AR blockers. Therefore, the development of better α_1 subtype-selective drugs to either block or enhance function with a minimum of side effects may help to combat subtype-related disorders.

To rationally design selective drugs, an understanding of subtype differences in the ligand-binding pockets would be invaluable. We recently described the α_1-AR ligand-binding pocket for agonists (13). With site-directed mutagenesis, selected putative ligand-binding residues in the α_{1b}-AR were converted, either individually or in combination, to the corresponding residues in the α_{1a}-AR. Mutation of two such residues (of ~172 amino acids in the TM domain) converted the agonist-binding profile entirely to that of the α_{1a}-AR. These two residues in the α_{1b}-AR, Ala204 and Leu314, are buried within the TM domains along with other key residues known to interact with the agonist, such as Asp125 and Ser207, which are involved in forming the counterion to the protonated amine and a hydrogen bond to the *meta*-hydroxyl of the catecholamine, respectively (14). All of these residues lay within the same plane of the modeled agonist-binding pocket. Thus, it seems that the binding site for agonists is located below the extracellular surface of the receptor, down into a pocket approximately one third of a TM spanning domain. This distance was estimated in the β_2-AR by fluorescent quenching experiments to be ≥11 Å deep (15).

To expand these types of studies for antagonist binding, we first generated an $\alpha_{1b/a}$ chimera of the fifth TM domain that also included a portion of the second extracellular loop. This α_{1b}-AR chimera displayed all of the higher binding affinity (8–29-fold) seen in the α_{1a}-AR for two antagonists, phentolamine and WB4101. Assessment of eight individual mutations from this region revealed that three residues located in the second extracellular loop contributed to the higher binding affinity. The data indicate that α_1 antagonists may not bind down within the TM domains and into a ligand-binding pocket as was previously described for agonists but rather may be analogous to the peptide hormone receptors that bind ligands near the surface or in the extracellular loops of the receptor.

Experimental Procedures

PCR-generated mutagenesis. Generation of the $\alpha_{1b/a}$ chimera was accomplished through PCR amplification of the rat α_{1a}-AR cDNA of the region corresponding to amino acids 177–208. Primers used were 5′-GAT GAG ACC GAA TGC GAG ATC AAT GAG GAG CCG GGC TAC-3′ (sense) and 5′-GGC TAC TAC GTA GAC TCG ACA GTA CAT AAC CAG AAT GAT-3′ (antisense) corresponding to the second extracellular loop portion of the rat α_{1a}-AR and a portion of the third intracellular loop, respectively. The sense primer incorporated a mismatch (*bold*) to encode a *Bsm*I restriction site (*underlined*) with correct sticky ends to anneal with the hamster α_{1b} *Bsm*I overhangs. The antisense primer encoded the native rat α_{1a} *Acc*I restriction site (*underlined*). PCR was then performed on 1 μg of rat α_{1a}-AR cDNA template with 40 pmol of each primer, 10 mM tricine, pH 8.0, 50 mM KCl, 0.01% gelatin, 200 μM concentrations of dNTPs, and 2.5 units of *Thermus aquaticus* DNA polymerase. The amplification profile, run for 40 cycles, consisted of 1 min at 95°, 2 min at 60°, and 3 min at 72°. The resulting DNA (130-bp fragment) was separated, digested with *Bsm*I and *Acc*I, and cloned into the *Bsm*I/*Acc*I sites of the hamster α_{1b}-cDNA, replacing the native fragment previously removed by restriction endonuclease digestion. The resulting construct was cloned into the expression vector pMT2′ (5) and sequenced to verify the chimera.

Site-directed mutagenesis. The construct used was the hamster α_{1b}-AR (4) or the rat α_{1a}-AR (2), which included a manufactured *Eco*RI restriction site at the 5′ end and a region encoding an octapeptide tag (i.d.4) at the end of the coding region that was used to evaluate membrane expression using a monoclonal antibody (anti-i.d.4). The attachment of this epitope after the coding region did not affect protein expression or the functional nature of the receptor. The construct ends with a stop codon and a *Not*I restriction site. The cDNAs were divided into two fragments by restriction endonucleases, and each fragment was inserted individually into M13mp19. This was done to reduce the potential incidence of spurious modifications in the DNA due to the M13 system as reported with large constructs (16). Site-directed mutagenesis was performed as previously described using the oligonucleotide-mediated double-primer method (16); this involves the use of a 20–25-base mutagenic primer encoding the codon mismatches to achieve the point mutation and the universal primer for extension on single-stranded M13 templates. After transformation of the extended products into DH5αF′ cells, plaques were screened for the mutation on nitrocellulose lifts by hybridization with the ^{32}P end-labeled mutagenic primer and then washed off the filter at 5° below the calculated T_m. The efficiency of mutagenic incorporation was 5% of total plaques. Positive plaques were purified, and the DNA was isolated and sequenced by the dideoxy method (Sequenase, Amersham, Arlington Heights, IL) to verify the mutation. The replicative form of the DNA was isolated from the M13, and the insert was removed and subcloned into the expression vector pMT2′. The full-length plasmid DNA was again sequenced to verify the mutation.

Cell culture and transfection. COS-1 cells (American Type Culture Collection, Rockville, MD) were grown in Dulbecco's modified Eagle's medium supplemented with 10% fetal bovine serum. cDNAs encoding the wild-type α_1-ARs and various mutants were subcloned into the mammalian expression vector pMT2′, as described previously (5). Plasmid DNA, purified by CsCl gradient centrifugation and Biogel A-50m (BioRad, Hercules, CA) column chromatography, was used to transfect cells. Transient expression in COS-1 cells was accomplished by the diethylaminoethane-dextran method (16). Cells were harvested at 60 hr after transfection.

Membrane preparation. COS-1 membranes were prepared as described previously (5). Membranes were prepared by washing the culture plates twice with warm Hanks' balanced salt solution. One milliliter of Hanks' balanced salt solution was added, and the plates were scraped and transferred to a 50-ml centrifuge tube. The intact cells were centrifuged at 1,000 × *g* in a Sorvall RT6000B rotor for 5 min, and the pellet was resuspended in 5 ml of 0.25 M sucrose. The cell suspension was centrifuged again at 1,000 × *g* for 5 min, and the pellet was resuspended in 10 ml of 0.25 M sucrose containing the following protease inhibitors: 20 μg/ml aprotinin, 20 μg/ml leupeptin, 20 μg/ml bacitracin, 20 μg/ml benzamidine, and 17 μg/ml phenylmethylsulfonyl fluoride. The cells were disrupted by N_2 cavitation and then homogenized in a Dounce homogenizer by 10 strokes with a tight-fitting (B)-type pestle. The mixture was then centrifuged at 1,260 × *g* for 5 min. Buffer (20 mM HEPES, pH 7.4, 12.5 mM $MgCl_2$, 1.4 mM EGTA) was added to the supernatant fraction, which was then centrifuged at 30,000 × *g* for 15 min. The resulting pellet was resuspended in 50 ml of buffer and recentrifuged for 15 min. The resulting pellet was resuspended in 1 ml of buffer containing 10% glycerol and stored in aliquots at −70°. The protein concentration was measured according to the method of Bradford (17).

Radioligand-binding. The ligand-binding characteristics of the expressed receptors were determined in a series of radioligand-binding studies using the α_1 antagonist radioligand [^{125}I]HEAT as described previously (5). Competition reactions (total volume, 0.25 ml) contained 20 mM HEPES, pH 7.5, 1.4 mM EGTA, 12.5 mM $MgCl_2$, 200 pM [^{125}I]HEAT, COS-1 membranes, and increasing amounts of unlabeled ligands known to interact with α_1-ARs. Nonspecific binding was determined in the presence of 10^{-4} M phentolamine. Reactions were stopped by the addition of cold HEPES buffer and were filtered onto Whatman GF/C glass-fiber filters with a Brandel cell harvester. Filters were washed five times with HEPES buffer, and bound radioactivity was determined using a Packard Auto-gamma 500 counter (Packard, Meriden, CT). Binding data were analyzed by the iterative curve-fitting program LIGAND (provided by Dr. Peter J. Munson, National Institutes of Health, Bethesda, MD). Hill coefficients were determined from the slope of the log-logit curve. For saturation binding studies, [^{125}I]HEAT concentrations of 25–800 pM were used. Saturation curves were obtained by incubating cell membranes with increasing amounts of [^{125}I]HEAT in the same buffer system used for the competition studies. To reduce interassay variation, binding assays were performed simultaneously with all constructs.

Molecular modeling. The coordinates of the α-carbon positions were determined by an overlay of the putative α_1-AR TM residues with the TM coordinates of bacteriorhodopsin (18) using data files generated using the Insight II molecular modeling software (Biosym Technologies, San Diego, CA). The boundaries of the putative TM domains were determined with an algorithm based on the weighted pairwise comparisons of adjacent residues (19). The α_1-AR model was then minimized, and conflicts were adjusted as described previously (20). Loop regions were generated separately and minimized after space-fixing the two amino acids at the TM boundaries. Assumptions of key amino acids involved in ligand binding, such as Asp125, are based on previous mutagenesis research and proposed models for the β-AR (21). Other α_1-AR residues shown (e.g., Ser207, Ser211) are based on previous mutagenesis work and the resulting models of the α_1-AR (14).

Materials. WB4101 and 5-methylurapidil were obtained from Research Biochemicals (Natick, MA); (+)-niguldipine was from Byk Gulden (Germany); (−)-epinephrine, methoxamine, oxymetazoline, phentolamine, and imidazole were from Sigma Chemical (St. Louis, MO); 2-aminomethylbenzodioxan was from Ryan Scientific (Columbia, SC); [^{125}I]HEAT was from DuPont-New England Nuclear (Boston, MA); and Biogel A-50m resin was from BioRad.

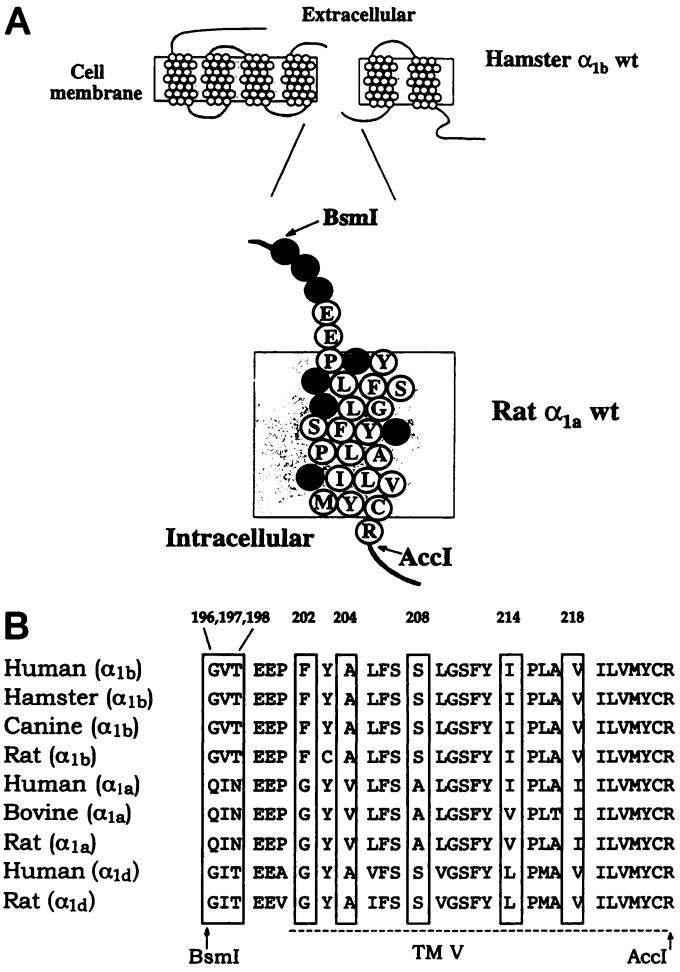

Fig. 1. *Top*, fifth TM domain of the rat α_{1a}-AR inserted into the hamster α_{1b} primary sequence. *Highlighted residues*, nonconserved between the two α_1 subtypes. *BsmI* and *AccI*, restriction sites within the hamster α_{1b} DNA sequence. *Bottom*, sequence alignment of the fifth TM domains of known α_1-ARs. *Boxed*, nonconserved amino acids not the result of species variation; *dotted line*, fifth TM spanning domain as predicted by an algorithm described in Experimental Procedures; *numbering of the amino acids*, based on the hamster α_{1b}-AR sequence; *wt*, wild-type.

Results and Discussion

The α_{1b}-AR and the α_{1a}-AR, although structurally similar in their TM domains, have some significant differences in their ligand-binding affinities for a number of agonists and antagonists. Determination of the critical amino acids responsible for these differences may assist in the design of better subtype-selective drugs. Previous work exploring the determinants of agonist selectivity between these two receptor subtypes revealed two amino acids in the TM spanning domains that accounted for the higher binding affinity seen in the α_{1a}-AR for three α_{1a}-selective agonists: oxymetazoline, cirazoline, and methoxamine (13). None of the eight initial mutations used in that study displayed changes in antagonist binding. To explore the determinants of antagonist binding, we first constructed a chimera (Fig. 1, *top*) between these two receptor subtypes to detect whether the fifth TM domain was involved. α_1 Antagonists are structurally diverse and are longer molecules compared with agonists but also have chemical similarities to a number of agonists. We rationalized that at least part of the antagonist structure would overlap with the agonist binding site. Because many residues (e.g., Ser188, Ser192, Val185) in the α_{1a}-AR fifth TM domain were found to interact with agonists (13, 14), we began our antagonist studies with this particular helix.

Analysis of the chimera. The $\alpha_{1b/a}$ chimera consists of the α_{1b}-AR with the fifth TM replaced with the corresponding region of the α_{1a}-AR (Fig. 1, *top*). Additional amino acids that represent a portion of the second extracellular and third intracellular loops were also replaced due to the convenience of restriction sites in those regions. The chimera was analyzed by its ability to bind a panel of agonists and antagonists. K_i values are shown in Table 1 and Fig. 2. The chimera had a 8–29-fold increased binding affinity for the α_{1a}-selective antagonists phentolamine and WB4101, a ligand-binding profile exactly like that of the wild-type α_{1a}-AR. 5-Methylurapidil, another α_{1a}-selective antagonist, also showed a significant 4-fold increased binding affinity with the chimera. However, because the chimera accounted for only a small fraction of the 17-fold selectivity in the α_{1a}-AR for 5-methylurapidil, we concentrated our studies on the two antagonists

TABLE 1

Ligand-binding profiles of wild-type α_{1b}-AR, α_{1a}-AR, and mutations

Competition binding studies were used to determine the K_i values (± standard error) of adrenergic ligands, as described in Experimental Procedures, using [^{125}I]HEAT as the radioligand and membranes prepared from COS-1 cells expressing the wild-type α_{1b}-AR, single or combination fifth TM α_{1b}-AR mutants, or the wild-type α_{1a}-AR. All competition binding isotherms (three experiments, performed in duplicate) were best fit to a single-site model. Receptor densities (B_{max}) were determined on the same membranes from equilibrium binding studies. **Bold** values indicate significant increases ($p < 0.05$) in affinity from the corresponding wild-type α_{1b}-AR (one-way analysis of variance followed by Student-Newman-Keuls multiple comparisons test).

	α_{1b}-AR	G196Q	V197I	T198N	F202G	A204V/S208A	I214V	V218I	Triple α_{1b}	Chimera	α_{1a}-AR
Antagonist											
Phentolamine	7.52 ± 0.02	**7.90 ± 0.05**	**7.88 ± 0.07**	**7.78 ± 0.05**	7.54 ± 0.04	7.41 ± 0.17	7.38 ± 0.04	7.55 ± 0.09	**8.32 ± 0.05**	**8.45 ± 0.05**	**8.41 ± 0.08**
WB4101	8.56 ± 0.04	**9.02 ± 0.09**	**9.24 ± 0.09**	**9.18 ± 0.12**	8.61 ± 0.01	8.47 ± 0.03	8.51 ± 0.03	8.73 ± 0.09	**10.19 ± 0.07**	**10.00 ± 0.10**	**10.02 ± 0.09**
(+)-Niguldipine	7.42 ± 0.21	N.D.	N.D.	N.D.	N.D.	7.71 ± 0.26	N.D.	N.D.	8.03 ± 0.04	7.57 ± 0.37	**8.77 ± 0.18**
5-Methylurapidil	7.28 ± 0.03	N.D.	N.D.	N.D.	N.D.	7.16 ± 0.16	N.D.	N.D.	N.D.	**7.87 ± 0.02**	**8.94 ± 0.05**
Agonist											
Oxymetazoline	6.16 ± 0.20	6.46 ± 0.06	5.99 ± 0.02	5.76 ± 0.03	N.D.	N.D.	N.D.	N.D.	6.28 ± 0.01	**7.67 ± 0.06**	**7.79 ± 0.03**
Epinephrine	5.82 ± 0.01	5.88 ± 0.11	6.12 ± 0.16	6.02 ± 0.06	N.D.	N.D.	N.D.	N.D.	6.26 ± 0.01	6.04 ± 0.06	6.06 ± 0.02
Methoxamine	3.40 ± 0.11	3.56 ± 0.06	3.74 ± 0.06	3.23 ± 0.01	N.D.	N.D.	N.D.	N.D.	3.61 ± 0.02	**3.95 ± 0.03**	**4.44 ± 0.08**
B_{max} (pmol/mg protein)	0.84	1.46	5.09	3.82	1.40	1.85	1.99	1.70	5.18	3.43	1.38
K_D (pM) [^{125}I]HEAT	43	46	34	29	70	60	26	35	34	23	29

N.D., not determined.

Fig. 2. Binding affinities for the $\alpha_{1b/a}$ chimera on α_{1a}-AR-selective antagonists. *x-axis*, the α_{1b}-AR (*WTb*) and the α_{1a}-AR (*WTa*) along with the initial chimera (*b/a Chimera*) composed of the hamster α_{1b} primary sequence backbone with the inserted rat α_{1a} fifth TM domain. *y-axis*, α_{1a}-selective antagonists. *z-axis*, binding affinity as K_i (−log). Values that were significantly different from the WTb are represented as *p* values determined by an analysis of variance followed by a Student-Newman-Keuls multiple-comparison test. Results are based on three or four experiments performed in duplicate. *WT*, wild-type.

that showed full selectivity. Another α_{1a}-selective antagonist, (+)-niguldipine, showed no significant changes from an α_{1b}-AR pharmacology (Fig. 2). The affinity of the chimera also did not change for the radioligand [^{125}I]HEAT (Table 1), a nonselective α_1 antagonist. The α_{1a}-selective agonists tested (i.e., oxymetazoline, methoxamine) (Table 1) displayed the 5–10-fold increased affinity, which was consistent with our previous results (12) that Val185 in the α_{1a}-AR fifth TM region was one of the residues responsible for agonist selectivity between these two receptor subtypes. The nonselective agonist (−)-epinephrine displayed no changes in affinity with the chimera.

Our results indicate that the chimera contains amino acids that are critical and sufficient in defining the antagonist binding pocket for phentolamine and WB4101 between the α_{1b}-AR and the α_{1a}-AR. The changes in pharmacology seem to be selective and the result of differences in amino acids that interact directly with both phentolamine and WB4101 and not the result of global changes in receptor conformation since the binding affinity for other α_1 agonists and antagonists were not affected.

Analysis of single mutations in converting the α_{1b}-AR to the α_{1a}-AR. The chimera contains eight different amino acids between the α_{1b}-ARs and α_{1a}-ARs (Fig. 1, *bottom*) that are not due to species variations. To find the specific amino acids that accounted for the higher binding affinity for the antagonists, individual mutations were generated and analyzed by their ability to bind phentolamine and WB4101. Rationalizing that the amino acids may lay within the TM domain as they did for agonist binding, we initially generated and analyzed only the five nonconserved amino acid residues in the fifth helix. As shown in Fig. 3, *top*, these five mutations (F202G, A204V, S208A, I214V, and V218I) demonstrated no significance difference in binding affinity for phentolamine or WB4101 from that of the wild-type α_{1b}-AR.

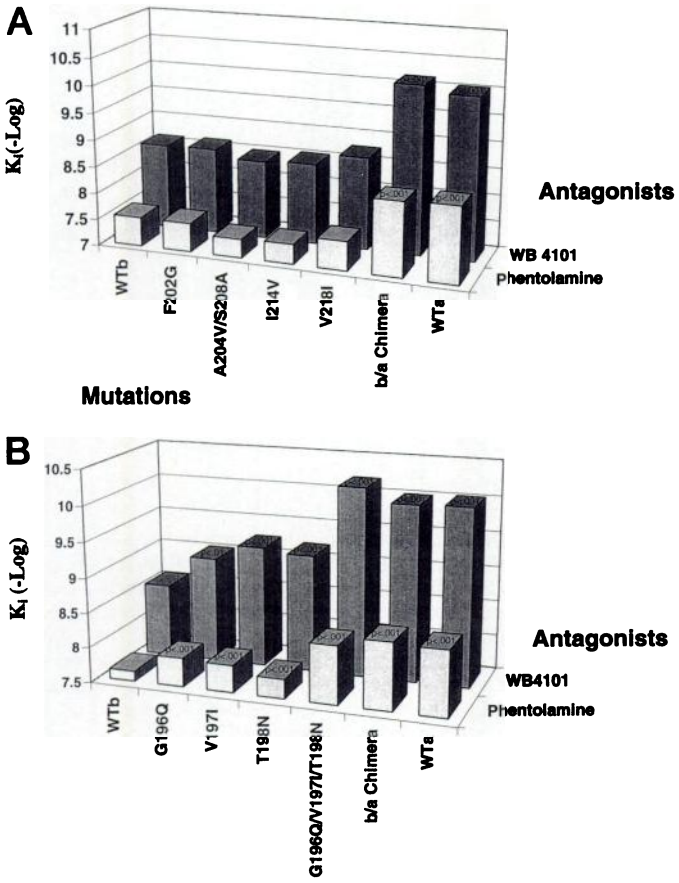

Fig. 3. *Top*, effects of the α_{1b}-AR fifth TM point mutations on the binding affinities for WB4101 and phentolamine. *Bottom*, effects of the α_{1b}-AR second extracellular loop point and combined mutations on the binding affinities for WB4101 and phentolamine. α_{1b}-AR mutations represent changing the amino acid in the α_{1b} at the designated amino acid number to the corresponding residue in the α_{1a}-AR subtype. *A204V/S208A*, double mutant in the fifth TM domain. *G196Q/V197I/T198N*, triple mutation in the α_{1b}-AR. Values that were significantly different from the WTb are represented as *p* values determined by an analysis of variance followed by a Student-Newman-Keuls multiple comparisons test. Results are based on three or four experiments performed in duplicate.

The remaining three point mutations located in the extracellular loop were then generated and analyzed. As shown in Fig. 3, *bottom*, all three point mutations (G196Q, V197I, T198N) individually increased in their binding affinity for both phentolamine (2–3-fold) and WB4101 (3–5-fold) toward that of the α_{1a}-AR. Thus, it seems that residues located near the surface of the receptor and likely in the second extracellular loop are responsible for some selective antagonist binding in the α_{1a}-AR.

Analysis of the triple α_{1b} mutation. A combination of the three point mutations that conferred antagonist selectivity were then combined into a single receptor (triple mutant, G196Q, V197I, T198N) to assess whether the individual mutations were independent and additive in their affects on changing the binding profiles to that of the α_{1a}-AR. As shown in Fig. 3, *bottom*, the triple mutation displayed similar affinities to both the $\alpha_{1b/a}$ chimera and the wild-type α_{1a}-AR for both phentolamine and WB4101. The three point mutations are synergistic in binding affinity when combined and thus likely represent three separate binding contacts with the antagonists. The increased affinity in the triple mutant fully accounts for all of the selective binding seen in the α_{1a}-AR for phentolamine (6-fold) and WB4101 (43-fold). All of the individual and combined α_{1b}-AR mutations produced changes in affinity for only phentolamine and WB4101. Three agonists tested [(−)-epinephrine, oxymetazoline, and methoxamine; the latter two are α_{1a} selective] did not change in their affinity for the 196, 197, and 198 point, or triple, mutation (Table 1), thus indicating the selectivity of these residues in antagonist binding is not due to aberrant folding/expression of the receptor as a result of mutational modification.

Reversing the mutations in the α_{1a}-AR. We performed the equivalent reverse mutations in the α_{1a}-AR to confirm that the three α_{1b} mutations G196Q, V197I, and T198N indeed define the critical residues differentiating the α_{1b}-AR and α_{1a}-AR antagonist binding pocket for phentolamine and WB4101 (Fig. 4). The results showed that the corresponding triple mutation in the α_{1a} (Q177G, I178V, N179T) completely reversed the binding affinity for phentolamine and WB4101 toward that of the α_{1b}-AR. Reversal of these mutations supports our hypothesis that these three residues located in the extracellular loop are the most critical determinants of the differences in antagonist binding between these two receptor subtypes.

Chemical mimicry in defining the antagonist-binding site. As a means of confirming our modeling and to discriminate between alternate approaches of docking the ligands in the receptor, we used smaller chemical mimics of discrete pharmacophores (i.e., imidazole, 2-aminomethylbenzodioxan; Fig. 5, *top*) in both phentolamine and WB4101 in separate competition ligand-binding studies with each individual mutation. Binding as a result of nonspecific sites is controlled by performing the competition studies jointly with the two wild-type and mutant receptors; thus, only binding that is due to selective interactions is apparent. As shown in

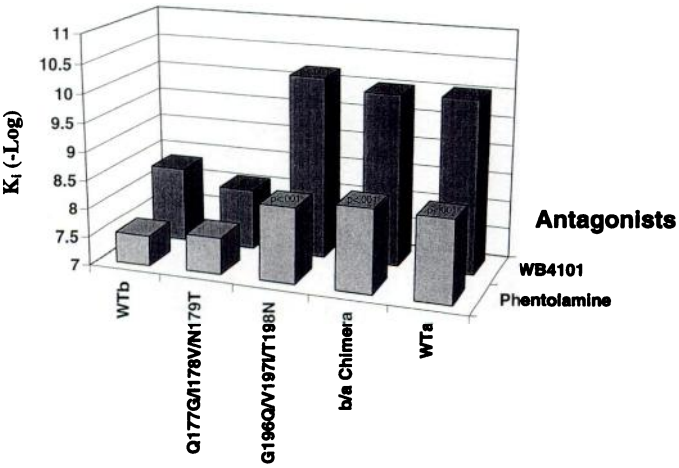

Fig. 4. Effects of reversing the mutations in the α_{1a}-AR on the binding affinities of WB4101 and phentolamine. *Q177G/I178V/N179T*, an α_{1a}-AR triple mutation in which amino acids were correspondingly mutated to α_{1b}-AR residues. *G196Q/V197I/T198N*, corresponding triple mutation in the α_{1b}-AR. Values that were significantly different from the WTb are represented as *p* values determined by an analysis of variance followed by a Student-Newman-Keuls multiple comparisons test. Results are based on three or four experiments performed in duplicate.

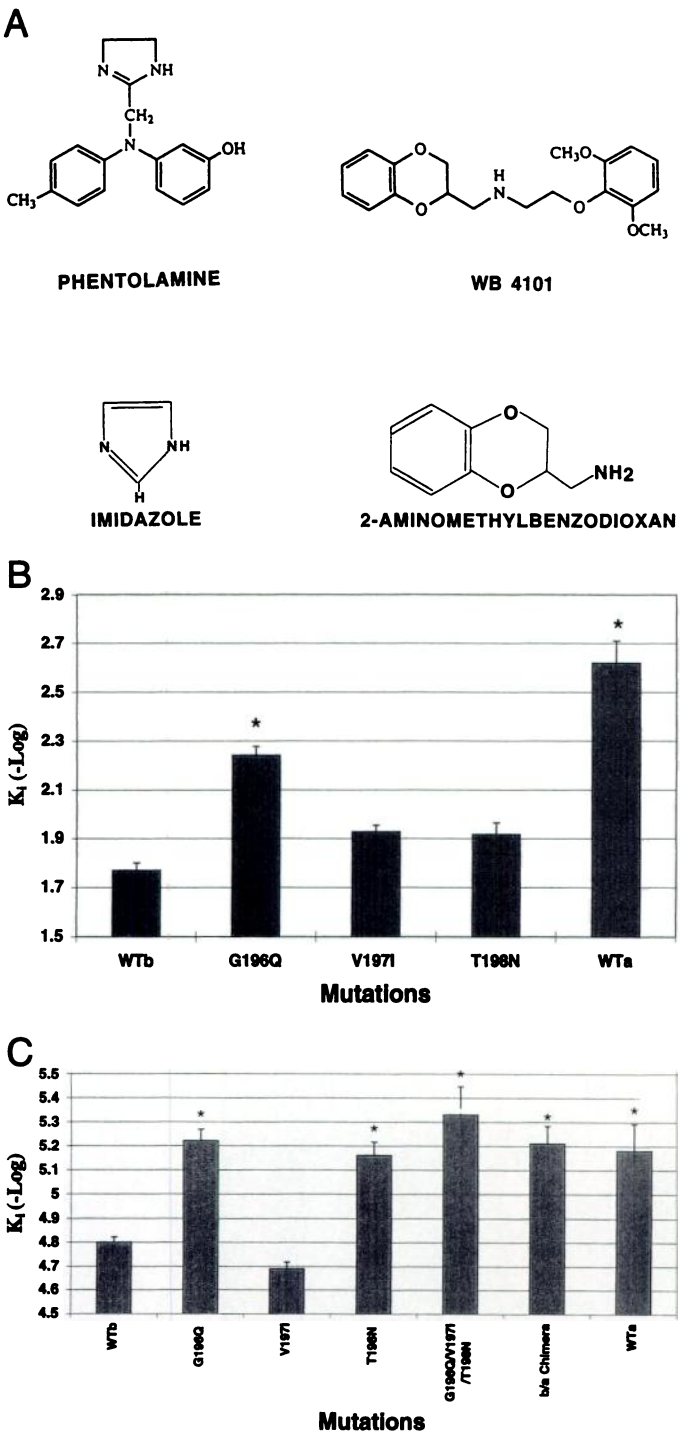

Fig. 5. *Top*, chemical structures of phentolamine, WB4101, and the chemical mimics imidazole and 2-aminomethylbenzodioxan. *Middle*, binding affinity of imidazole on the wild-type receptors and the α_{1b}-AR point mutations. Competition binding studies were used to determine K_i values as described in Experimental Procedures using [^{125}I]HEAT as the radioligand and membranes prepared from COS-1 cells expressing the wild-type receptors or α_{1b}-AR point mutations. All competition binding isotherms were best fit to a single-site model. *Bottom*, binding affinity of 2-aminomethylbenzodioxan on the wild-type and mutated receptors. *G196Q/V197I/T198N*, triple mutation in the α_{1b}-AR. *, $p <$ 0.01, significantly different from the WTb (B and C); determined by an analysis variance followed by a Student-Newman-Keuls multiple comparisons test. Results are based on three or four experiments performed in duplicate.

Fig. 5, *middle*, the imidazole compound that mimics part of the structure of phentolamine can directly compete with [^{125}I]HEAT binding with a homogeneous population of binding sites. The imidazole compound shows selectivity (6-fold) for the wild-type α_{1a}-AR compared with the wild-type α_{1b}-AR, suggesting that more than half of the selectivity seen in the α_{1a}-AR for phentolamine is due to this chemical moiety. Imidazole also selectively binds to only one of the α_{1b}-AR point mutations, G196Q, suggesting that this residue is significantly involved in its binding. A chemical mimic of WB4101, 2-aminomethylbenzodioxan (Fig. 5, *top*), was also selective (3-fold) for the G196Q and T198N mutants (Fig. 5, *bottom*). No significant differences from the wild-type α_{1b}-AR were seen for the V197I mutant. The triple α_{1b}-AR mutant and b/a chimera showed no significant differences from the wild-type α_{1a}-AR or the 196 and 198 mutant receptors. Although both these chemical mimics display low affinity for these receptors because of their size and thus do not display synergism of binding that is apparent in the triple mutation compared with the individual mutations for the intact antagonists (Fig. 3, *bottom*, versus Fig. 5, *bottom*), there still is selective binding with particular mutations that is consistent with expected interactions; i.e., 2-aminomethylbenzodioxan shows selectivity for the α_{1a} versus α_{1b} wild-type receptors as well as the triple-mutant and chimeric receptor consistent with WB4101 selectivity. This suggests that the use of these chemical mimics is a valid approach to discriminating alternative dockings, although it is not certain whether these smaller molecules bind in a similar orientation as the intact antagonist. However, the data suggest the importance of the 196 residue position and its interaction with the imidazoline group of phentolamine. The 196 and 198 residue positions interacted with functional moieties on the benzodioxan portion of WB4101.

Modeling the antagonist binding site for phentolamine and WB4101. Previous analysis of the subtype specificity between the β_1- and β_2-AR using an extensive number of chimeras expressed in *Escherichia coli* (22) suggested that each of 11 selective ligands (both agonists and antagonists) binds to its own subsite. Similar studies between these β-AR subtypes localized selective agonist binding to the fourth TM (23). However, no single residue substitution seemed to be capable of altering the subtype specificity of the receptor. No extracellular loop residues were mutated in these receptors, especially in determination of antagonist selectivity. In contrast, the α_1-ARs may have more discernible and distinct binding interactions that are capable of resolving to specific amino acid residues. Our previous study of agonist selectivity between the α_{1b}- and α_{1a}-ARs identified two critical amino acids that accounted for all of the selectivity differences for available agonists (13). In our current study, we focused on antagonist selectivity, which also indicated discreet amino acid interactions.

Based on our data, we are able to suggest models of the two α_1 subtype differences in their antagonist-binding pockets. In the α_{1a}-AR for phentolamine binding (Fig. 6A), Gln196 seems to form a hydrogen bond with the imidazoline nitrogen. Gln196 was positioned in this manner to concur with the chemical mimicry studies. Based on this interaction, the other two amino acids positioned themselves consistently as follows. Ile197 forms a hydrophobic interaction with the methyl substituent of the phenyl ring. Ile197 may, however,

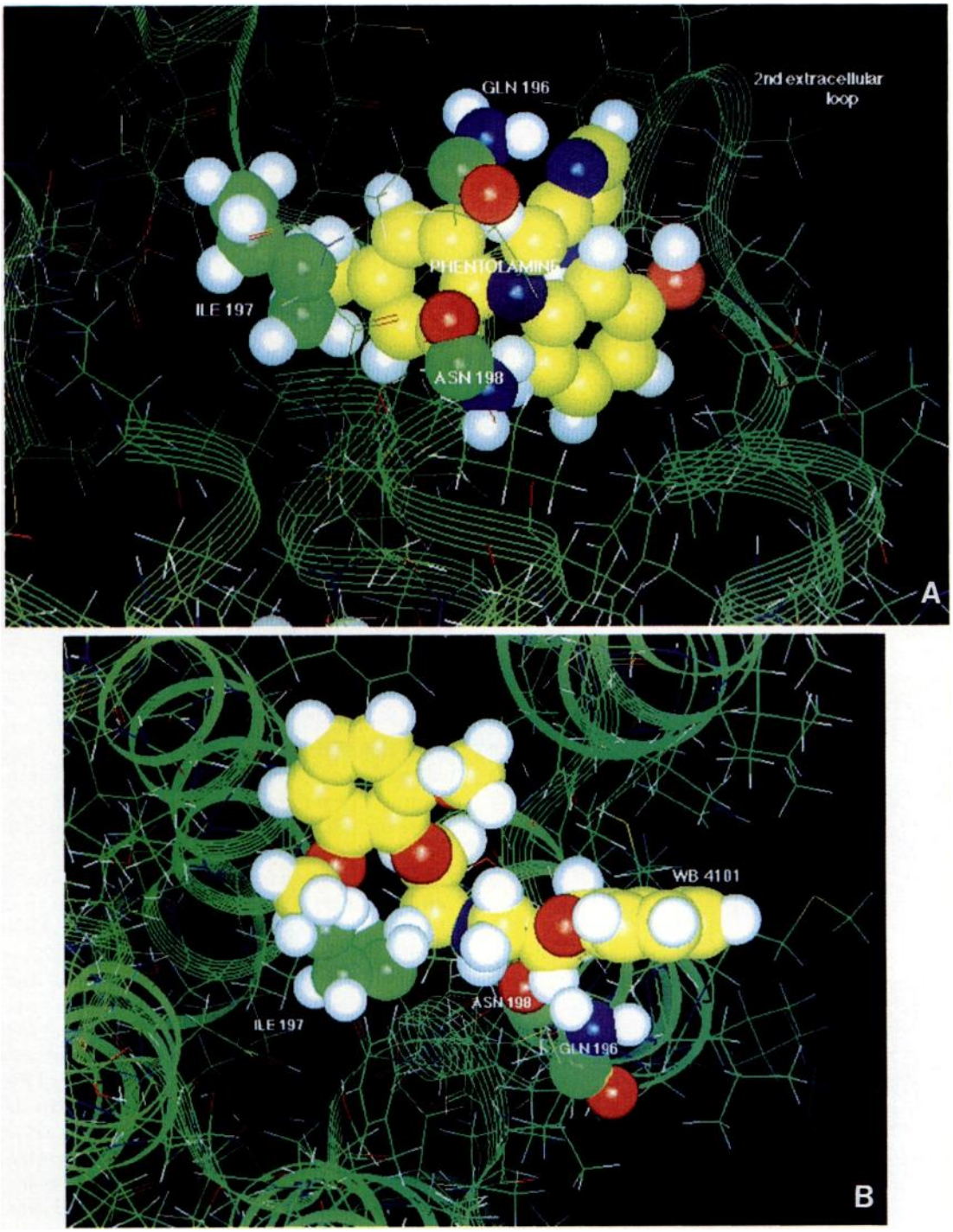

Fig. 6. A, side-view model of the α_{1b}-AR showing the docking of phentolamine in the mutated second extracellular loop. Gln196 seems to form a hydrogen bond with the imidazoline nitrogen. Ile197 forms a hydrophobic interaction with the methyl substituent of the phenyl ring. Ile197 may, however, interact with the ring itself. Asn198 is in a position to hydrogen bond with the nitrogen atom that links the three ring structures. B, top-view model of the α_{1b}-AR showing the docking of WB4101 in the mutated second extracellular loop. Gln196 forms a hydrogen bond with the dioxan oxygen, Ile197 forms a hydrophobic contact with the methoxy group from the other phenyl ring, and Asn198 from below hydrogen bonds with the nitrogen linker. C, full-view model of the α_{1b}-AR showing the position of phentolamine in the extracellular loops and its relationship to the TM surface. D, alternate full-view model of the α_{1b}-AR showing the possible position of WB4101 and its relationship to the TM surface. Part of the antagonist structure would be located within the TM spanning domains if the second extracellular loop folds down close to the surface of the receptor. The fourth TM has been removed to allow better visualization of the binding pocket. Asp125, Ser207, and Ser211 represent the position of the critical point contacts involved in agonist binding in the α_1-ARs as described previously (14). Asp125 forms a counterion to the protonated amine of catecholamines, whereas the serine residues are involved in agonist binding with the catechol hydroxyls. Only Ser207 of the two serine residues, however, is sufficient in receptor activation.

interact with the ring itself. Asn198 is in a position to hydrogen bond with the nitrogen atom that links the three ring structures. WB4101 was likewise positioned to concur with the 2-aminomethylbenzodioxan competition studies. For WB4101 binding (Fig. 6B), Gln196 forms a hydrogen bond with a dioxan oxygen, Ile197 forms a hydrophobic contact

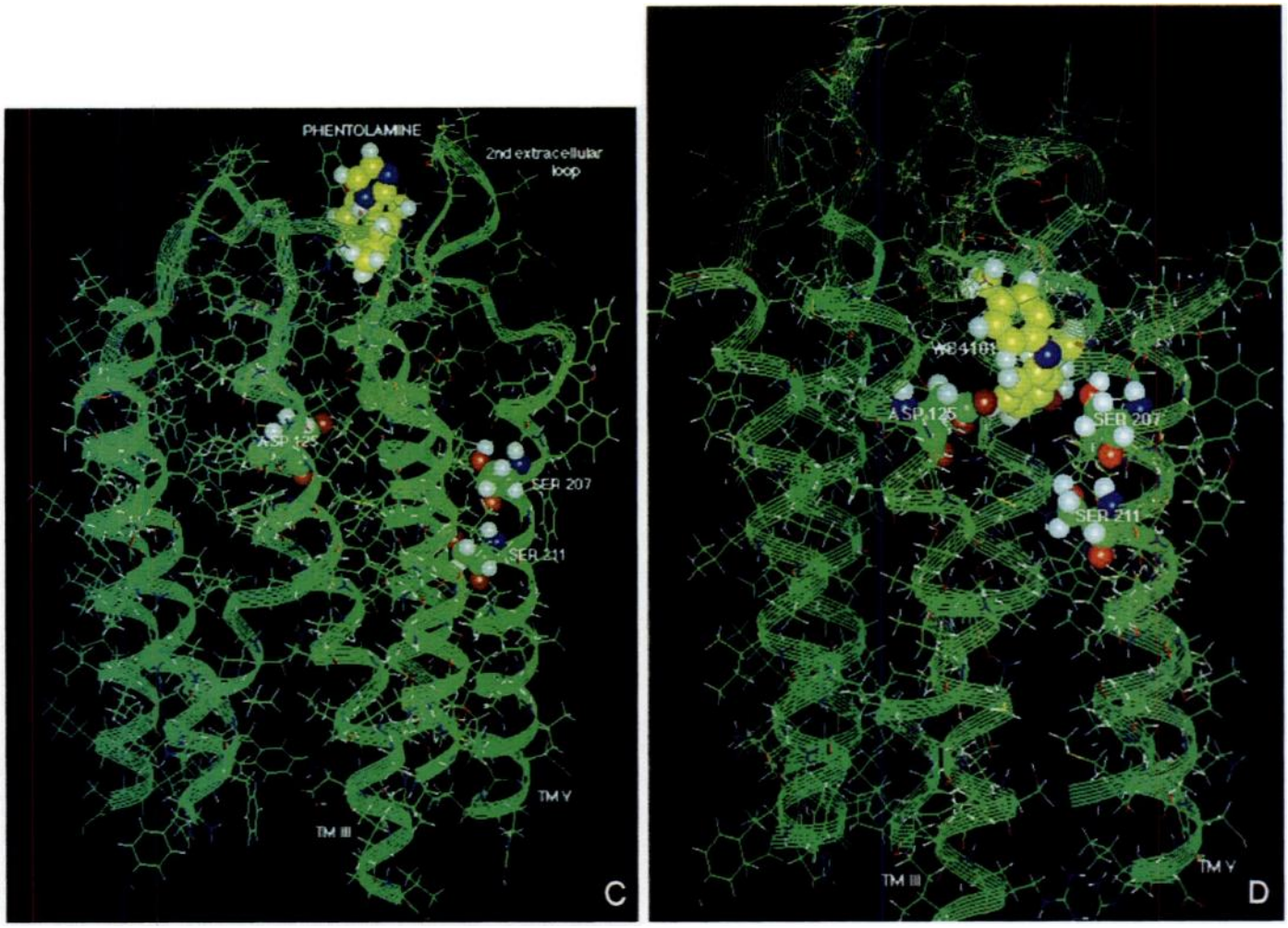

Fig. 6. c,d

with the methoxy group from the phenyl ring, and Asn198 from below hydrogen bonds with the nitrogen linker. These three residues in combination differentiate the antagonist-binding pocket of the α_{1b}- and α_{1a}-AR for these particular ligands. Other conserved residues between the two α_1 subtypes (in particular, aromatic residues) located in the extracellular loops or at the TM surface may interact with the aromatic rings of these antagonists and account for the remainder of the high binding affinity that is nonselective for these ligands.

It seems likely that these three residues are indeed located in the extracellular loop and are not part of the TM domain. Although the boundaries of the hydrophobic helices in the membrane are uncertain, an algorithm that predicts the boundaries has placed these residues in the extracellular loop (19). In addition, these three residues are also located on the extracellular side of a glycine and proline residue followed by two glutamic acid residues in the putative second extracellular loop (QINEEPG-TMV). The glycine and proline would likely terminate the α helix, and the three critical residues are located in a hydrophilic area of the loop.

Because the structures, if any, of the extracellular loops themselves are unknown, the position of the antagonist-binding pocket is still speculative but has essentially two scenarios. If the second extracellular loop is folded away from the TM domains and out into the hydrophilic environment, the binding of phentolamine and WB4101 as represented in Fig. 6C, may be exclusively in the extracellular loops and positioned well above the TM surface. However, it is possible that the second extracellular loop is folded down toward the TM surface (Fig. 6D), in which case, part of the antagonist binds with other TM residues located near the extracellular surface of the receptor. Proline residues are located on both termini of the second extracellular loop at the TM boundaries and may affect the folding pattern. It seems unlikely that the second extracellular loop is folded down toward the surface in the unliganded state because this would block accessibility to the agonist-binding pocket located within the TM domains. More likely, the loop may move or fold during the process of antagonist docking. Experiments to differentiate these potential binding modes are currently under way.

We have defined three important residues that are critical and sufficient in differentiating the ligand-binding pocket for phentolamine and WB4101 between the two α_1-AR subtypes. We are able to model the interaction and in doing so provided a rational basis for the design of better subtype-selective drugs based on these known antagonists. It is interesting that these residues involved in selectivity are located in an

extracellular loop and may be the mode by which some antagonists bind in the biogenic amine receptors. Although previous work in the β-AR has suggested that antagonists bind in a similar pocket to agonists, many of these antagonists were designed or synthesized from agonist structures. α_1-AR antagonists are quite diverse in structure, and each may bind uniquely and in a dissimilar mode than agonists. The antagonist-binding mode may be similar to that observed in the peptide hormone receptors, such as angiotensin (24), endothelin (25), and neurokinin (26), that have critical binding determinants located on extracellular loops or at the extracellular surface of the receptor. Specifically, the neurokinin receptor binds a nonpeptide antagonist at the fifth TM surface, a residue positioned only three or four amino acids away from our model. Although α_1 antagonists are not as large as the peptide hormones, they are similar in size to the nonpeptide antagonists. Thus, it may seem that some antagonists of the α_1-ARs bind the receptor in the extracellular loops or near the surface of the receptor and not down into a pocket formed by the TM domains, as was previously determined for the α_1 agonists.

References

1. Hieble, J. P., D. B. Bylund, D. E. Clarke, D. C. Eikenburg, S. Z Langer, R. J. Lefkowitz, K. P. Minneman, and R. R. Ruffolo. International Union of Pharmacology, X: recommendation for nomenclature of α_1-adrenoceptors: consensus update. *Pharmacol. Rev.* **47**:267–270 (1995).
2. Perez, D. M., M. T. Piascik, N. Malik, R. Gaivin, and R. M. Graham. Cloning, expression, and tissue distribution of the rat homolog of the bovine α_{1c}-adrenergic receptor provide evidence for its classification as the α_{1a} subtype. *Mol. Pharmacol.* **46**:823–831 (1994).
3. Schwinn, D. A., J. N. Lomasney, W. Loreng, P. J. Szklut, R. T. Fremeau, T. L. Yang-Feng, M. G. Caron, R. J. Lefkowitz, and S. Cotecchia. Molecular cloning and expression of the cDNA for a novel α_1-adrenergic receptor subtype. *J. Biol. Chem.* **265**:8183–8189 (1990).
4. Cotecchia, S., D. A. Schwinn, R. R. Randell, R. J. Lefkowitz, M. G. Caron, and B. K. Kobilka. Molecular cloning and expression of the cDNA for the hamster α_1-adrenergic receptor. *Proc. Natl. Acad. Sci. USA* **85**:7159–7163 (1988)
5. Perez, D. M., M. T. Piascik, and R. M. Graham. Solution-phase library screening for the identification of rare clones: isolation of an α_{1d}-adrenergic receptor cDNA. *Mol. Pharmacol.* **40**:876–883 (1991)
6. Lomasney, J. W., S. Cotecchia, W. Lorenz, W. Y. Leung, D. A. Schwinn, T. L. Yang-Feng, M. Braunstein, R. J. Lefkowitz, and M. G. Caron. Molecular cloning and expression of the cDNA for the α_{1a}-adrenergic receptor. *J. Biol. Chem.* **266**:6365–6369 (1991).
7. Piascik, M. T., R. D. Guarino, M. S. Smith, E. E. Soltis, D. L. Saussy, Jr., and D. M. Perez. The specific contribution of the novel *alpha*-$_1$d adrenoceptor to the contraction of vascular smooth muscle. *J. Pharmacol Exp. Ther.* **275**:1583–1589 (1995).
8. King, H. K., A. S. Goetz, S. D. C. Ward, and D. L. Saussy, Jr. AH11110A is selective for the α_{1b} subtype of α_1-adrenoceptors. *Soc. Neurosci. Abstr.* **20**:A526 (1994)
9. Giardina, D., M. Crucianelli, C. Melchiore, C. Taddei, and R. Testa. Receptor binding profile of cyclazosin, a new α_{1b}-adrenoceptor antagonist. *Eur. J. Pharmacol.* **287**:13–16 (1995).
10. Simpson, P. Norepinephrine-stimulated hypertrophy of cultured rat myocardial cells is an alpha$_1$-adrenergic response. *J. Clin. Invest.* **72**:732–738 (1983) .
11. Lepor, H., S. Auerbach, A. Puras-Baez, P. Narayan, M. Soloway, F. Lowe, T. Moon, G. Leifer, and P. Madsen. A randomized, placebo-controlled multicenter study of the efficacy and safety of terazosin in the treatment of benign prostatic hyperplasia. *J. Urol.* **148**:1467–1474 (1992).
12. Forray, C., J. A. Bard, J. M. Wetzel, G. Chiu, E. Shapiro, R. Tang, H. Lepor, P. R. Hartig, R. L. Weinshank, T. A Branchek, and C. Gluchowski. The α_1-adrenergic receptor that mediates smooth muscle contraction in human prostate has the pharmacological properties of the cloned human α_{1c} subtype. *Mol. Pharmacol.* **45**:703–708 (1994).
13. Hwa, J., R. M. Graham, and D. M. Perez. Identification of critical determinants of α_1-adrenergic receptor subtype selective agonist binding. *J. Biol. Chem.* **270**:23189–23195 (1995).
14. Hwa, J., and D. M. Perez. The unique nature of the serine interactions for α_1-adrenergic receptor agonist binding and activation. *J. Biol. Chem.* **271**:6322–6327 (1996).
15. Tota, M., and C. D. Strader. Characterization of the binding domain of the *beta*-adrenergic receptor with the fluorescent antagonist carazolol: evidence for a buried ligand binding site. *J. Biol. Chem.* **265**:16891–16897 (1990).
16. Sambrook, J., E. F. Fritsch, and T. Maniatis. *Molecular Cloning: A Laboratory Manual*. Cold Spring Harbor Laboratory, Cold Spring Harbor, NY (1989).
17. Bradford, M. M. A rapid and sensitive method for the quantitation of microgram quantities of protein utilizing the principle of protein-dye binding. *Anal. Biochem.* **72**:248–254 (1976).
18. Henderson, R., J. M. Baldwin, T. A. Ceska, F. Zemlin, E. Beckmann, and K. H. Downing. Model of the structure of bacteriorhodopsin based on high-resolution electron cryo- microscopy. *J. Mol. Biol.* **213**:899–929 (1990).
19. Reik, R. P., N. D. Handshumacher, S.-S. Sung, M. Tan, M. J. Glynias, M. D. Schluchter, J. Novotny, and R. M. Graham. Evolutionary conservation of both the hydrophilic and hydrophobic nature of transmembrane residues. *J. Theor. Biol.* **172**:245–258 (1995)
20. Sung, S.-S., N. D. Handshumacher, J. Novotny, and R. M. Graham. Molecular model of the hamster α_{1b}-adrenergic receptor. *FASEB J.* **5**:A804 (1991).
21. Strader, C. D., I. S. Sigal, R. B. Register, M. R. Candelore, E. Rands, and A. F. Dixon. Identification of residues required for ligand binding to the β-adrenergic receptor. *Proc. Natl. Acad. Sci. USA* **84**:4384–4388 (1987).
22. Marullo, S., L. J. Emorine, A. D. Strosberg, and L. Delavier-Klutchko. Selective binding of ligands to β_1, β_2 or chimeric β_1-, β_2-adrenergic receptors involves multiple subsites. *EMBO J.* **9**:1471–1476 (1990).
23. Dixon, R. A., W. S. Hill, M. R. Candelore, E. Rands, R. E. Diehl, M. S. Marshall, I. S. Sigal, and C. D. Strader. Genetic analysis of the molecular basis for *beta*-adrenergic receptor subtype specificity. *Proteins* **6**:267–274 (1989).
24. Feng, Y.-H., K. Noda, Y. Saad, X.-P. Liu, A. Husain, and S. S. Karnik. The docking of Arg^2 of angiotensin II with Asp^{281} of AT_1 receptor is essential for full agonism. *J. Biol. Chem.* **270**:12846–12850 (1995).
25. Adachi, M., Y. Y. Yang, A. Trezeciak, Y. Furuichi, and C. Miyamoto. Identification of a domain of ET_A receptor required for ligand binding. *FEBS Lett.* **311**:179–183 (1992).
26. Fong, T. M., M. A. Cascieri, H. Yu, A. Bansal, C. Swain, and C. D. Strader. Amino-aromatic interaction between histidine 197 of the neurokinin-1 receptor and CP 96345. *Nature (Lond.)* **362**:350–353 (1993).

Send reprint requests to: Dr. Dianne M. Perez, FF3-01, Department of Molecular Cardiology, The Cleveland Clinic Foundation, 9500 Euclid Avenue, Cleveland, OH 44195. E-mail: perexd@cesmtp.ccf.org